Asian Journal of Chemistry; Vol. 33, No. 4 (2021), 903-908

ASIAN JOURNAL OF CHEMISTRY

https://doi.org/10.14233/ajchem.2021.23106

Effect of Ce^{3+} Co-doping on $GdPO_4$:Tb^{3+} Nanoparticles: Photoluminescence and Energy Transfer Studies

N. YAIPHABA

P.G. Department of Chemistry, D.M. College of Science, Imphal-795001, India

Corresponding author: E-mail: ningombam.y@gmail.com

Received: 27 December 2020; *Accepted*: 16 February 2021; *Published online*: 20 March 2021; AJC-20302

Low temperature synthesis of Tb^{3+}-doped $GdPO_4$ nanoparticles sensitized with Ce^{3+} (Ce^{3+} = 0, 3, 5, 7 and 10 at.%) have been reported. Ethylene glycol was used as capping agent as well as reaction medium at 160 ºC. The as-prepared particles crystallized in a monoclinic structure with an average crystallite size of 25-46 nm. From the photoluminescence study, enhanced emission of Tb^{3+} with co-doping of Ce^{3+} was attributed to efficient energy transfer from the sensitizer to activator. The luminescence emission intensity increases upto 5 at.% of Ce^{3+} and then decreases. Less efficient energy transfer from sensitizer to the activator with increasing concentration of sensitizer may be attributed to critical concentration of Ce^{3+} with the host or dipole-quadrupole interaction amongst the Ce^{3+} ions. Moreover, presence of -OH group in the samples will make them a potential target for biological labeling and optical devices.

Keywords: Nanoparticles, Photoluminescence, Ethylene glycol, Sensitizer, Energy transfer.

INTRODUCTION

In recent years, inorganic nanomaterials activated by lanthanide has find wide applications in fiber-optic communications [1], blue LED-based solid state lighting [2], lighting & display [3,4], biological labelling/drug delivery [5,6], *etc*. The wider applications of these crystalline phosphor nanomaterials over the bigger or micron sized particles may be attributed to the higher surface to volume atom ratio and quantum confinement effect [7]. In case of lanthanides because of their well shielded 4*f*-electrons, 4*f*-4*f* transitions gives sharp absorption lines and long decay life time with excellent coherence properties [8,9]. In addition these, lanthanides ions have emission range from ultraviolet to infrared region and presence multi energy level makes energy transfer amongst them possible. Due to this reason nanoparticles doped with lanthanide ions have been widely studied [2,4,10-17].

Rare earth phosphate ($REPO_4$) nanoparticles, doped with lanthanides ions have emerged as an important candidate for optoelectronic devices and biological fluorescence labeling [4,8,14,15]. They have excellent luminescence, long decay time, low toxicity, high chemical and photochemical stability, resistance to photochemical degradation and large Stokes shift [10, 14]. At present, one of the important focus on these nanoposphor is on improving the luminescence intensity by co-doping of appropriate sensitizer in the different host material. The sensitizers absorb energy strongly and transfer to the excited state of activators efficiently.

$GdPO_4$ is an important host matrix for luminescent lanthanide ion doped nanophosphors having multi functional nanoplatforms. Earlier we have reported $GdPO_4$ as a potential host where efficient energy transfer from gadolinium ion (Gd^{3+}), due to large absorption cross section ($^8S_{7/2} \rightarrow {}^6I_{11/2}$ transition) in the ultraviolet region, to activator ions (Eu^{3+}, Tb^{3+}, Dy^{3+}, *etc*.) [15,18-20]. However, further enhancement of luminescence intensity can be normally achieved by co-doping a suitable sensitizer such as Ce or Bi into the host matrix. There have been report on Ce enhance luminescent host materials such as $LaPO_4$:Dy [21], YAG:Sm [22], $LaPO_4$:Tb^{3+} nanorods [8], $NaCeF_4$ [23], Y/La/GdF_3 [24], Ce^{3+}, Dy^{3+}/Tb^{3+} doped $BaZn_2(PO_4)_2$ phosphors [23], *etc*. using different synthesis methods (taru paper). However, only few literature are reported on Ce codoped $GdPO_4$:Tb nanophospor [25,26].

Hence, the present study deals with the low temperature synthesis and luminescence properties of Ce^{3+} and Tb^{3+} doped $GdPO_4$ nanoparticles using ethylene glycol as solvent. The low

temperature synthesis, using ethylene glycol helps to stabilize the nanoparticles and thereby, without using any moisture sensitive reagents, hydrothermal conditions and long chain organic molecules as stabilizing ligands. Also photoluminescence study have been undertaken to confer the energy transfer process. These stabilized nanoparticles are dispersible in aqueous/organic solvents (water and ethanol) allowing for developing polymer/sol-gel based luminescent materials and display devices.

EXPERIMENTAL

Sample preparations: Nanoparticles of $GdPO_4$ and 10 at.% Tb^{3+} doped $GdPO_4$ codoped with Ce^{3+} (Ce^{3+} = 1,3, 5, 7 and 10 at.%) were prepared using ethylene glycol (Merck) as both capping agent and reaction medium at 160 ºC. Gadolinium oxide (99.99%, Aldrich), terbium nitrate (99.99%, Alfa Aesar), ammonium dihydrogen phosphate (99.999%, Aldrich) and cerium carbonate (99.999%, Alfa Aesar) were used as sources of Gd^{3+}, Tb^{3+} and PO_4^{3-} and Ce^{3+}, respectively.

In a typical synthesis of 10 at.% $Tb^{3+}$and 2 at.% Ce^{3+} doped $GdPO_4$ nanoparticles, 500 mg of Gd_2O_3, 67 mg of $Tb(NO_3)_3$ and 17 mg of $Ce(NO_3)_3$ were dissolved together in dilute HCl acid in a 100 mL round bottom flask. Excess HCl was removed by evaporating several times with double distilled water. To this reaction medium, 50 mL of ethylene glycol and 360 mg of $NH_4H_2PO_4$ were added. The reflux was carried out at 160 ºC for 3 h. The precipitate formed was separated by centrifugation at 12,000 rpm, washed several times with acetone and dried in ambient atmosphere. The same procedure was followed for the preparation of all other doped samples by taking stoichiometric amounts.

The reactions occured between M^{3+} and PO_4^{3-} are as follows:

$$2M^{3+} + 6Cl^- \longrightarrow 2Gd/CeCl_3 + 3H_2O$$

$$MCl_3 + (NH_4)H_2PO_4 \longrightarrow MPO_4 + NH_4Cl + 2HCl$$

(M^{3+}= Gd^{3+}, Ce^{3+} and Tb^{3+})

Characterization: Structural analysis of the as-prepared Ce^{3+}/Tb^{3+}:$GdPO_4$ samples were done using a PANalytical powder diffractometer (X'Pert PRO) with CuKα radiation (λ = 0.15405 nm) with Ni filter. X Ray diffraction (XRD) patterns were recorded from 10º to 70º (2θ) for 30 min. The FT-IR spectra of the Ce^{3+}/Tb^{3+} :$GdPO_4$ samples were recorded using a SHIMADZU (model 8400 S) spectrometer by making thin pellets with KBr. A Perkin-Elmer (LS-55) luminescence spectrometer in phosphorescence mode equipped with xenon discharge lamp as the excitation source is used to record all the photoluminescence spectra and lifetime measurements of the samples. Pulse width at half height is < 10 μs. For the lifetime measurements gate time was fixed at 0.05 ms and the delay time was varied starting from 0.1 ms. All the measurements were taken at room temperature.

RESULTS AND DISCUSSION

XRD study: The XRD patterns of as-prepared Ce^{3+} codoped 10 at.% Tb^{3+} doped $GdPO_4$ (Ce^{3+} = 0, 5 and 10 atom.%) are given in Fig. 1. The diffraction patterns of the as-prepared nanoparticles were matched with the monoclinic $GdPO_4$ structure (JCPDS No. 32-0836). The similarities in the XRD patterns indicate the homogenous substitution of Ce^{3+} and Tb^{3+} into the Gd^{3+} sites of $GdPO_4$ nanoparticles. It is attributed to the similar ionic radii of Tb^{3+} (1.095 Å), Ce^{3+} (1.196 Å) and Gd^{3+} (1.107 Å) in a nine coordinated system, making $GdPO_4$ a suitable host/matrix for incorporation of lanthanide ions [26]. The substitution of the Tb^{3+} into the Gd^{3+} sites of $GdPO_4$ nanoparticles has been elaborately discussed and reported elsewhere [15]. The average crystallite sizes are calculated using Debye-Scherrer equation ($d = 0.9\lambda/\beta\cos\theta$) and are found to be in range of 25-46 nm (Table-1) for all doped samples and are in agreement with the TEM study [15]. Here, particles are assumed to be spherical in shape and its diameter is considered as crystallite size.

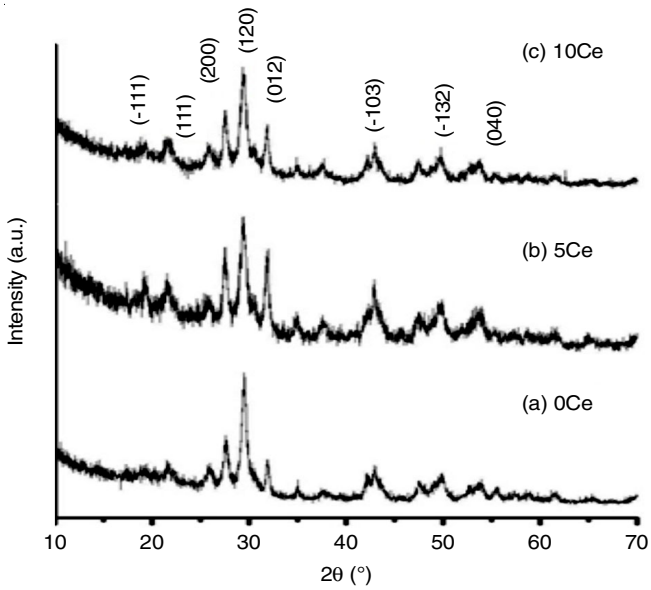

Fig. 1. XRD patterns of as-prepared $GdPO_4$:Tb^{3+} (at.% 10) co-doped with Ce^{3+} (a) 0 at.%, (b) 5 at.% and (c) 10 at.%

TABLE-1
CRYSTALLITE SIZE AND DECAY LIFE TIME OF 10 at.% Tb^{3+}: $GdPO_4$: CO-DOPED WITH DIFFERENT Ce^{3+} CONCENTRATION (at.%)

Ce^{3+} (conc.)	Crystallite size (nm)	Time (min)
0	32	3.1
1	41	3.2
3	46	3.7
5	25	3.4
7	39	3.2
10	42	2.9

IR studies: The Fourier transform IR spectra of Ce^{3+} codoped 10 at.% Tb^{3+}:$GdPO_4$ (Ce = 0, 1, 3, 5, 7, 10 at.%) nanoparticles are shown in Fig. 2. Prominent peaks at 554, 577, 630, 879, 951, 1069, 1458, 1670, 2861, 2931 and 3299 cm^{-1} are observed. From the $(PO_4)^{3-}$ group symmetry, band regions are assigned as ν_1, ν_2, ν_3 and ν_4, respectively [15,25,27]. The frequency bands ν_3 and ν_4 are due to the stretching and bending vibrations of IR active modes while ν_1 and ν_2 are due to Raman active modes. The bands at 554, 577and 630 cm^{-1} were assigned as ν_4 region are for bending vibrations of PO_4^{3-}. Whereas, the

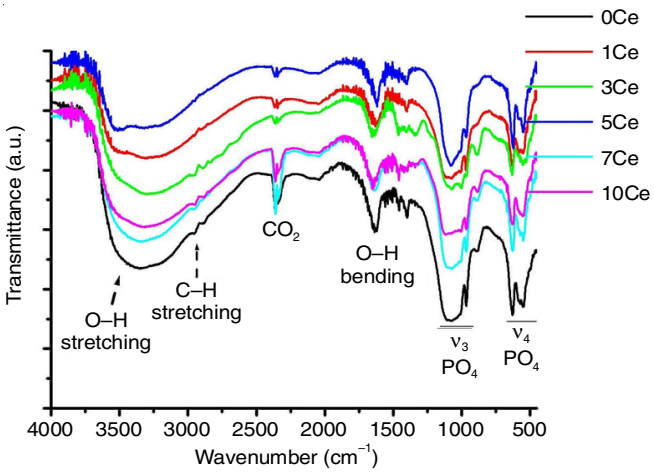

Fig. 2. IR spectra of as-prepared $GdPO_4$:Tb^{3+} (at.%) co-doped with Ce^{3+}

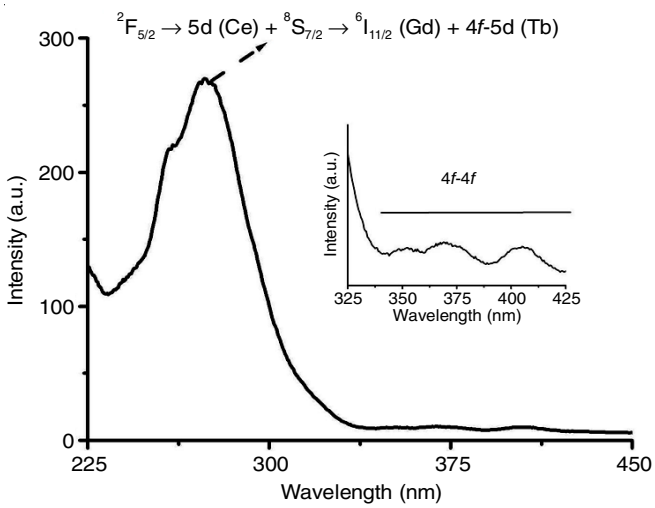

Fig. 3. Excitation spectra of 5 at.% Ce^{3+} co-doped $GdPO_4$:Tb (10 at.%) monitoring emission at 545 nm

bands at 879, 951 and 1069 cm^{-1} were assigned as ν_3 region, which is due to the stretching vibrations of PO_4^{3-} [25,27]. Similar peaks are reported in previous studies on $LnPO_4$ (Ln = Gd, Y, La) [21-23,25-27]. Peaks at 1670 and 3299 cm^{-1} correspond to bending and stretching vibrations, respectively for O-H group of ethylene glycol molecule, which is used as capping agent for nanoparticles [15,25,26,28]. The presence of hydrogen bond in ethylene glycol molecules is indicated by the broad band at 3299 cm^{-1} [15]. Water associated with $GdPO_4$ could not be distinguished as the O-H peaks due to water have been merged with those of ethylene glycol. The peaks at 2856 and 2927 cm^{-1} correspond to the stretching vibrations of CH_2 group of ethylene glycol molecule whereas, its bending vibration (scissoring) was observed at 1460 cm^{-1} [15,26]. The peak at 2362 cm^{-1} is due to absorption of CO_2 gas from atmosphere on the surface of particles. The IR study suggests as-prepared Ce^{3+} and Tb^{3+} doped $GdPO_4$ nanoparticles, have -OH group the samples will be re-dispersible in water and ethanol, which will make them a potential target for biological labeling. Again, due to the re-dispersible properties such nanoparticles can also be incorporated into polyvinyl alcohol polymer and this film will be useful in optical devices [15].

Luminescence study: Excitation spectra of 10 at.% doped Tb^{3+}:$GdPO_4$ sensitized with 5 at.% Ce^{3+}monitoring emission at 545 nm is shown in Fig. 3 and (inset) expanded region from 325 to 425 nm. The excitation spectrum consists of broad peaks with maxima at 273, and a hump at 258 nm. These two peaks are associated with 4*f*-5*d* transitions, which are spin allowed of Ce^{3+} from ground state $^2F_{5/2}$ of 4*f* to 5*d* excited state. The spin forbidden 4*f*-4*f* transition of Ce^{3+} at 315 nm and Gd^{3+} at 278 nm could not be observed separately as merged with spin allowed transition of Ce^{3+}. The small excitation peaks at 350, 369 and 405 nm (inset) corresponds to $^7F_6 \rightarrow {}^5G_5$, $^7F_6 \rightarrow {}^5L_{10}$, $^7F_6 \rightarrow {}^5G_6$ to *4f-4f* transitions of Tb^{3+} [10,29,30]. The presence of strong excitation peak over 4*f*-4*f* transition indicates the occurrence of energy transfer process from Ce^{3+} and Gd^{3+} to Tb^{3+} ion. It is to be noted that second harmonic generation of 545 nm will give ~273 nm. In order to verify, another excitation spectrum of 5 at.% Ce^{3+} doped 10 at.% Tb^{3+}:$GdPO_4$ monitoring emission at 488 nm and keeping filter at 395 nm was also carried out (not shown). In this case, second harmonic generation of 488 nm will give peak at 244 nm, but was not observed. Still, the same excitation peak position at 274 nm is obtained, thus confirmed that excitation peak at 274 nm is genuine.

Photoluminescence emission spectra of 5 at.% Ce^{3+} doped 10 at.% Tb^{3+}:$GdPO_4$ at different excitation wavelengths of 258, 273, 350, 369 and 405 nm are shown in Fig. 4. From the spectra several emission lines at 489, 545, 587 and 621 nm were observed and the peaks correspond to $^5D_4 \rightarrow {}^7F_6$ (489 nm), $^5D_4 \rightarrow {}^7F_5$ (545 nm), $^5D_4 \rightarrow {}^7F_4$ (587 nm) and $^5D_4 \rightarrow {}^7F_3$ (621 nm) transitions of Tb^{3+} [15,31]. The peaks at 489 nm and 545 nm correspond to the electric dipole and magnetic dipole allowed transitions, respectively. Among the various emission bands, the strongest emission was obtained at 545 nm giving rise to the green emission for Tb^{3+}. The emission bands of the peaks excited at 273 and 258 nm is highly intense than when excited at 350, 369, 405 nm excitation, suggesting a strong energy transfer to the excited states of Tb^{3+} from Gd^{3+}/Ce^{3+}. The energy transfer follows the Foster-Dexter energy transfer theory, if two fluorophors are within a critical distance (~20 Å) and the donor's emission

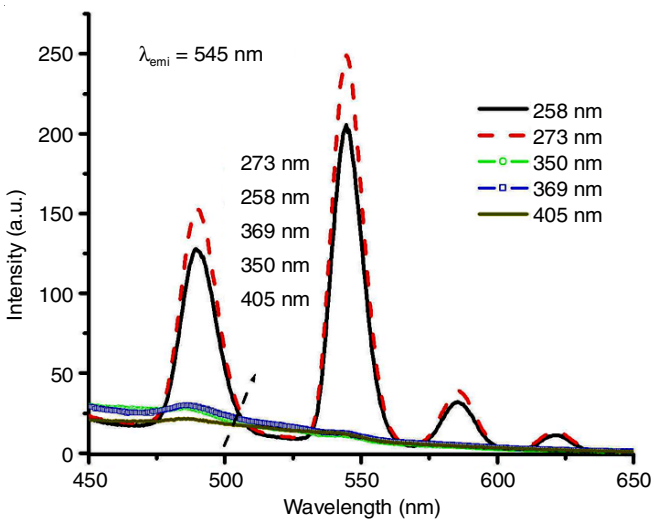

Fig. 4. Emission spectra of 5 at.% Ce^{3+} co-doped $GdPO_4$:Tb^{3+} (10 at.%) at different excitation wavelengths 258, 273, 35, 369 and 405 nm

overlapped with the acceptor's absorption bands, than transfer of energy takes place from donor to activator [32,33]. A schematic diagram of energy transfer between Ce^{3+}/Gd^{3+} to Tb^{3+} is shown in Fig. 5.

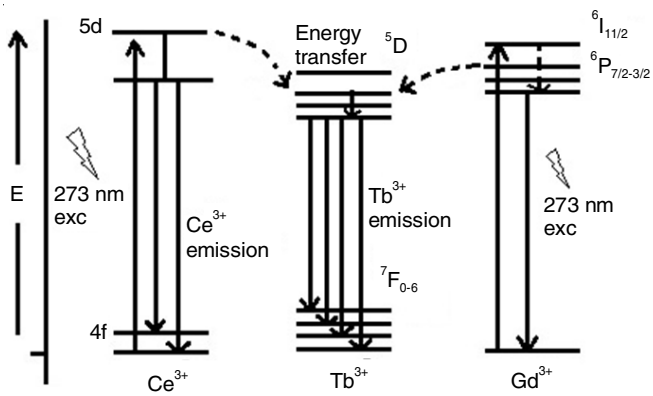

Fig. 5. Schematic diagram of energy transfer process in Tb^{3+}/Ce^{3+}:$GdPO_4$

In order to observe the changes in the emission intensity for different concentrations of Ce^{3+}, emission spectra of Ce^{3+} doped 10 at.%Tb^{3+}:$GdPO_4$ (Ce^{3+} = 0, 1, 3, 5, 7, 10 at.%) were recorded after excitation at 273 nm (Fig. 6). The emission intensity of Tb^{3+} increases as Ce^{3+} concentration increases from 3 to 5 at.% and then decreases with further increase of Ce^{3+}. A decrease in the intensity emission intensity of Tb^{3+}:$GdPO_4$ with increasing Ce^{3+} ion concentrations might be due to critical concentration of Ce^{3+} with the host or dipole-quadrupole interaction amongst the Ce^{3+} ions. A critical concentration of Ce^{3+} absorption cross-section from 250-290 nm (Ce^{3+}/Gd^{3+} absorption) are maximum with highest probability of energy transfer to Tb^{3+}. A net effect in the absorption as well as emission process was observed with the simultaneous increase and Ce^{3+} and Gd^{3+} ion. Thus, above 7 at.% Ce^{3+} a decrease in emission intensity of Ce^{3+}/Tb^{3+} was observed due to critical concentration or dipole-quadrupole interaction.

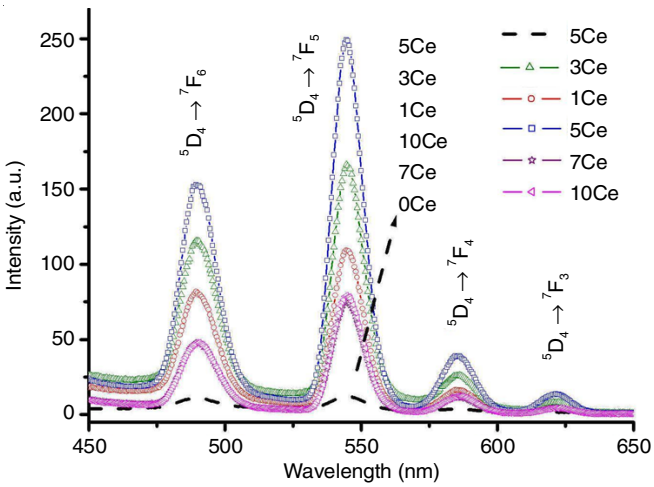

Fig. 6. Emission spectra of $GdPO_4$:Tb^{3+} co-doped with Ce^{3+}(Ce^{3+} = 0, 1, 3, 5, 7, 10 at.%) monitoring excitation at 273 nm

Lifetime study: Fig. 7 shows the normalized photoluminescence decays for of $GdPO_4$:10 at.%Tb^{3+} codoped with

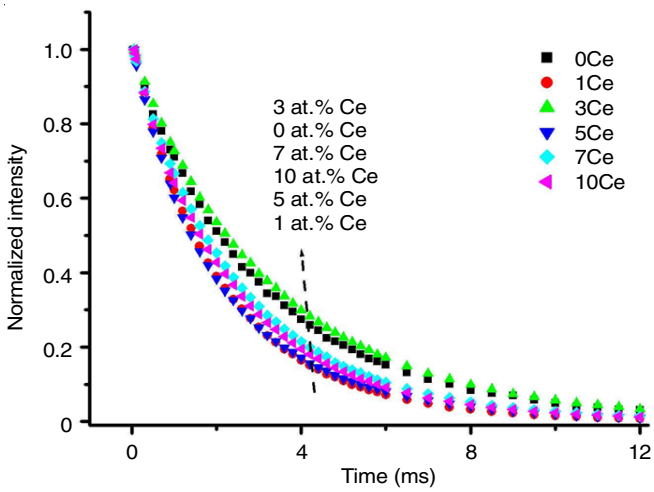

Fig. 7. Normalized luminescence decays of 10 at.% doped Tb^{3+}:$GdPO_4$ co-doped with Ce^{3+} (Ce^{3+} = 0, 1, 3, 5, 7 and 10 at.%) samples after excitation at 274 nm and monitoring emission at 545 nm

Ce^{3+}(Ce^{3+} = 0, 1, 3, 5, 7 and 10 at.%) after excitation at 274 nm and monitoring the emission at 544 nm. Decay data were fitted with monoexponential equations (Fig. 8). For the monoexponential decay fit, it is expressed as:

$$I = I_0 \exp\left(-\frac{t}{\tau}\right) \quad (1)$$

where I_o and I are intensities at zero time and at time t, respectively, and τ is the lifetime for transition. This was carried out by considering following assumptions [15,16]:

(i) Homogeneous distribution of Tb^{3+} ions in the host matrix, and

(ii) Tb^{3+} ions may be located closer to surface due to strong ligand-Tb^{3+} interaction and strong quenching effect at higher concentrations.

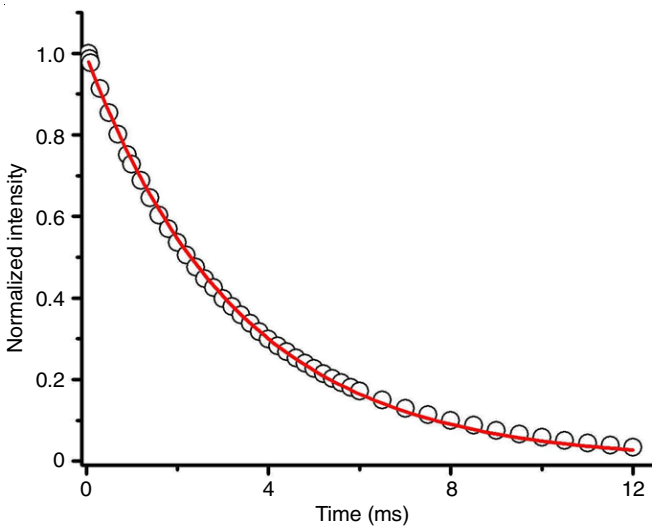

Fig. 8. Decay data are fitted with monoexponential equations for Ce^{3+} co-doped $GdPO_4$:Tb

The ln I *vs*. time plots are shown in inset of Fig. 9, where I stands for luminescence intensity. As the concentration of Ce^{3+} in Ce^{3+} co-doped 10 at.% Tb^{3+}:$GdPO_4$ increases above 5 at.%,

the lifetime decreases (Table-1). This behaviour is attributed to due to critical concentration or dipole-quadrupole interaction of the Ce^{3+} ion as discuss earlier. The lifetimes varies from 3.1 to 3.7 ms for Ce^{3+} doped 10 at.% Tb^{3+}:$GdPO_4$ nanoparticles (Ce^{3+} = 0, 1, 3, 5, 7 and 10 at.%).

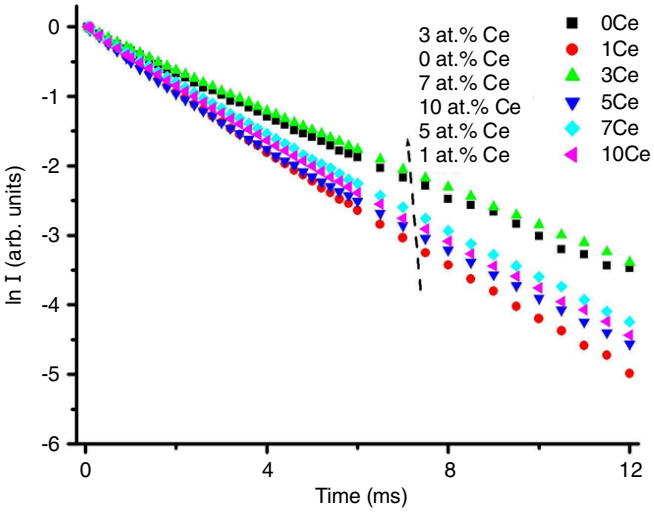

Fig. 9. ln (I) *vs.* time plot for luminescence decays of 10 at.% doped Tb^{3+}: $GdPO_4$ co-doped with Ce^{3+} (Ce^{3+} = 0, 1, 3, 5, 7 and 10 at.%) samples after excitation at 274 nm and monitoring emission at 545 nm

Conclusion

The Ce^{3+} and Tb^{3+} doped $GdPO_4$ nanoparticles were synthesized and their luminescence properties have been investigated. For the different excitation wavelengths, the most prominent emission was observed at 273 nm excitation, showing efficient energy transfer from Ce^{3+} and Gd^{3+} to Tb^{3+}. The luminescence intensity increases manifold with the doping of Ce^{3+} and increases up to 5 at.% Ce^{3+} and then decreases as the dopant concentration of Ce^{3+} increases. This may be due to critical concentration of Ce^{3+} with the host or dipole-quadrupole interaction amongst the Ce^{3+} ions. Moreover, as-prepared Ce^{3+} and Tb^{3+} doped $GdPO_4$ nanoparticles, have -OH group the samples will be re-dispersible in water and ethanol, which will make them a potential target for biological labeling and optical devices.

ACKNOWLEDGEMENTS

The author thanks Prof. N. Rajmuhon Singh, Manipur University, Imphal, India for his support.

CONFLICT OF INTEREST

The authors declare that there is no conflict of interests regarding the publication of this article.

REFERENCES

1. D.B. Barber, C.R. Pollock, L.L. Beecroft and C.K. Ober, *Opt. Lett.*, **22**, 1247 (1997); https://doi.org/10.1364/OL.22.001247
2. A. Gautam and F.C.J.M. van Veggel, *Chem. Mater.*, **23**, 4817 (2011); https://doi.org/10.1021/cm202139u
3. T. Jüstel, H. Nikol and C. Ronda, *Angew. Chem. Int. Ed.*, **37**, 3084 (1998); https://doi.org/10.1002/(SICI)1521-3773(19981204)37:22<3084::AID-ANIE3084>3.0.CO;2-W
4. N.S. Singh, N.K. Sahu and D. Bahadur, *J. Mater. Chem. C Mater. Opt. Electron. Devices*, **2**, 548 (2014); https://doi.org/10.1039/C3TC31586J
5. E. Beaurepaire, V. Buissette, M.-P. Sauviat, D. Giaume, K. Lahlil, A. Mercuri, D. Casanova, A. Huignard, J.-L. Martin, T. Gacoin, J.-P. Boilot and A. Alexandrou, *Nano Lett.*, **4**, 2079 (2004); https://doi.org/10.1021/nl049105g
6. J.Y. Park, M.J. Baek, E.S. Choi, S. Woo, J.H. Kim, T.J. Kim, J.C. Jung, K.S. Chae, Y. Chang and G.H. Lee, *ACS Nano*, **3**, 3663 (2009); https://doi.org/10.1021/nn900761s
7. A.P. Alivisatos, *Science*, **271**, 933 (1996); https://doi.org/10.1126/science.271.5251.933
8. Y. Liu, D. Tu, H. Zhu, R. Li, W. Luo and X. Chen, *Adv. Mater.*, **22**, 3266 (2010); https://doi.org/10.1002/adma.201000128
9. T.T. Taru Chanu, N. Yaiphaba and N.R. Singh, *Ceram. Int.*, **43**, 10239 (2017); https://doi.org/10.1016/j.ceramint.2017.05.051
10. G. Phaomei, R.S. Ningthoujam, W.R. Singh, R.S. Loitongbam, N.S. Singh, A. Rath, R.R. Juluri and R.K. Vatsa, *Dalton Trans.*, **40**, 11571 (2011); https://doi.org/10.1039/c1dt11264c
11. N.R. Singh and N.G. Singh, eds.: S.J. Dhoble, V.B. Pawade, H.C. Swart and V. Chopra, Spectroscopy of Lanthanide-Doped Oxide Materials, Woodhead Publishing, Elsevier, UK, Chap. 5 (2019).
12. K. Riwotzki, H. Meyssamy, A. Kornowski and M. Haase, *J. Phys. Chem. B*, **104**, 2824 (2000); https://doi.org/10.1021/jp993581r
13. E.M. Goldys, K. Drozdowicz-Tomsia, S. Jinjun, D. Dosev, I.M. Kennedy, S. Yatsunenko and M. Godlewski, *J. Am. Chem. Soc.*, **128**, 14498 (2006); https://doi.org/10.1021/ja0621602
14. R. Meenambal, P. Poojar, S. Geethanath, T.S. Anitha and S. Kannan, *J. Biomed. Mater. Res.*, **107**, 1372 (2019); https://doi.org/10.1002/jbm.b.34229
15. N. Yaiphaba, R.S. Ningthoujam, N.R. Singh and R.K. Vatsa, *Eur. J. Inorg. Chem.*, **2010**, 2682 (2010); https://doi.org/10.1002/ejic.200900968
16. J.W. Stouwdam and F.C.J.M. van Veggel, *Nano Lett.*, **2**, 733 (2002); https://doi.org/10.1021/nl025562q
17. H. Bai, Y. Yang, J. Bao, A. Wu, Y. Qiao, X. Guo, M. Wang, W. Li, Y. Liu and X. Zhu, *R. Soc. Open Sci.*, **7**, 192235 (2020); https://doi.org/10.1098/rsos.192235
18. J. Dexpert-Ghys, R. Mauricot and M.D. Faucher, *J. Lumin.*, **69**, 203 (1996); https://doi.org/10.1016/S0022-2313(96)00094-4
19. G. Phaomei and N. Yaiphaba, *Adv. Nano Res.*, **3**, 55 (2015); https://doi.org/10.12989/anr.2015.3.2.055
20. N. Yaiphaba, R.S. Ningthoujam, N. Shanta Singh, R.K. Vatsa and N. Rajmuhon Singh, *J. Lumin.*, **130**, 174 (2010); https://doi.org/10.1016/j.jlumin.2009.08.008
21. L. Wang, M. Xu, H. Zhao and D. Jia, *New J. Chem.*, **40**, 3086 (2016); https://doi.org/10.1039/C5NJ03148F
22. F.N. Sayed, V. Grover, S.V. Godbole and A.K. Tyagi, *RSC Adv.*, **2**, 1161 (2012); https://doi.org/10.1039/C1RA00651G
23. X. Qu, H.K. Yang, G. Pan, J.W. Chung, B.K. Moon, B.C. Choi and J.H. Jeong, *Inorg. Chem.*, **50**, 3387 (2011); https://doi.org/10.1021/ic1022467
24. H. Sun, X. Zhang and Z. Bai, *J. Rare Earths*, **31**, 231 (2013); https://doi.org/10.1016/S1002-0721(12)60263-4
25. N.K. Sahu, R.S. Ningthoujam and D. Bahadur, *J. Appl. Phys.*, **112**, 014306 (2012); https://doi.org/10.1063/1.4731644
26. R.D. Shannon, *Acta Crystallogr. A*, **32**, 751 (1976); https://doi.org/10.1107/S0567739476001551
27. N.K. Sahu, N.S. Singh, L. Pradhan and D. Bahadur, *Dalton Trans.*, **43**, 11728 (2014); https://doi.org/10.1039/C4DT00792A

28. K. Nakamoto, Infrared and Raman Spectra of Inorganic and Coordination Compounds, ed. 5, Wiley: New York (1986).
29. C. Peng, C. Li, G. Li, S. Li and J. Lin, *Dalton Trans.*, **41**, 8660 (2012); https://doi.org/10.1039/c2dt30325f
30. R.S. Ningthoujam, eds.: S.B. Rai and Y. Dwivedi, Enhancement of Photoluminescence by Rare Earth Ions Doping in Semiconductor Inorganic, Nova Science Publishers Inc.: USA (2012).
31. K. Kömpe, H. Borchert, J. Storz, A. Lobo, S. Adam, T. Möller and M. Haase, *Angew. Chem. Int. Ed.*, **42**, 5513 (2003); https://doi.org/10.1002/anie.200351943
32. J.R. Lakowicz, Principles of Fluorescence Spectroscopy, Kluwer Academic/Plenum Publishers: New York (1999).
33. D.L. Dexter, *J. Chem. Phys.*, **21**, 836 (1953); https://doi.org/10.1063/1.1699044